

Article

Thrust Prediction of an Active Flapping Foil in Waves Using CFD

Rupesh Kumar  and Hyunkyong Shin *

Widetank, School of Naval Architecture and Ocean Engineering, University of Ulsan, Ulsan 44610, Korea; rupesh7243@gmail.com

* Correspondence: hkshin@ulsan.ac.kr; Tel.: +82-52-259-2696

Received: 18 September 2019; Accepted: 4 November 2019; Published: 6 November 2019



Abstract: A horizontally submerged passive flapping foil can generate thrust force against the wave propagation using wave energy. This renewable method has been used for the design of propulsion and maneuvering systems of ships and other floating structures. Recently, the passive flapping foils were applied to design the station-keeping system of deep-water floaters. Studies proved that the passively flapping foil system was ineffective in short waves and drift of the floater beyond the design limit was recorded. Therefore, an active flapping foil was investigated as a potential solution to this problem. A computational fluid dynamics (CFD) numerical tool “ANSYS Workbench 19.2” was used to predict the thrust force generated by the active flapping foil in a short wave. Results proved that the active flapping foil can effectively convert wave energy into propulsive energy in short waves and the magnitude of the thrust force depends on the flapping frequency.

Keywords: Active; flapping; foil; thrust; CFD

1. Introduction

The flapping of wings and tails are common and have inspired several researchers to carry out experiments to understand the behavior of the flapping motion in a fluid. Several kinds of research have been done in the past for ship propulsion using wave energy [1,2]. The hydrofoils were attached to the ship through an elastic system, so that the hydrofoil can oscillate in the heave and pitch directions to effectively generate the thrust force against the wave propagation.

Wu [3] introduced a two-dimensional hydrofoil that can extract energy by oscillating through waves in water. It was found that energy can be extracted only when the wave had a vertical velocity component to the hydrofoil span and if the flow was uniform, energy could not be extracted. Finally, the best mode of heave and pitching for extraction of wave energy by passive type wave devouring propulsor was obtained.

Later, Wu’s theory of an oscillating hydrofoil was extended by including a free surface effect to study the passively flapping hydrofoil, famously known as wave devouring propulsion [4,5]. Extensive experimental work on the pure pitch and pure heave with NACA 0015 can be found in [6]. Further, heave and pitch motions were combined for NACA 0012 and the performance of flapping foil propulsion were experimentally studied [7]. Subsequently, the effects of angle of attack on the flapping foil propulsion were reported [8]. Studies show that the explicit control of the angle of attack in flapping foil propulsion can broadly increase thrust force and efficiency. The application of flapping foil for maneuvering was also reported [9]. It was found that by adding pitch bias to the harmonic motion, large lift force can be achieved. Also, flapping foil as an auxiliary propulsor near the free surface was reported [10,11]. Recently, passive flapping foils and plates were installed around a floater to investigate the stationkeeping using wave energy experimentally [12]. This report showed that the passive flapping system was very effective in long and mid waves, however, in short waves,

passive flapping system could not keep the floater in the allowable drift limit. Probably the energy extracted by the flapping system in short waves was not enough to keep the position of the floater and external energy must be applied. Therefore, an investigation of the active mode of a flapping system becomes important.

For the past few years, due to technical advancements in the field of computational fluid dynamics (CFD), the numerical analysis has become more realistic and can be done in a reasonable time frame. Also, CFD can be coupled with the computational structural mechanics (CSM) to simulate several multi-physics problems such as fluid-structure interaction (FSI). In recent years, FSI simulations have been conducted to evaluate the environmental loads and dynamic response of the offshore structures [13–15] and many aerodynamic [16,17] and biomedical applications [18,19].

The purpose of this study was to investigate the possibilities of using flapping foils for designing a station-keeping system of a floater in short waves. In order to do that, the evaluation and comparison of thrust forces of each foil in active and passive modes were necessary. In the passive mode, the flapping of hydrofoil was governed by the incoming waves, therefore, thrust extents could not be controlled by flapping frequencies, there were the other means to do it. However, in the active mode, hydrofoil was driven by an electric motor that could generate various flapping frequencies, therefore, a controller must be designed to effectively operate the flapping frequencies of hydrofoil to meet the station-keeping goals. In order to do that, thrust forces must be estimated for each operating motor frequency in short waves and still water conditions. Therefore, in this study, a flapping foil was set to oscillate at a fixed location and the thrust forces were evaluated for the active mode of flapping foil in still water and short waves for five operating flapping frequencies. Also, the CFD model was validated by comparing the thrust forces generated by fixed foil and passive flapping foil.

2. Methodology

This paper aimed to analyze the fluid-structure interaction of a horizontally placed active flapping foil in short waves. A rigid NACA 0015 section of 8 cm chord length, made of acrylic glass was attached from its leading edge to the 0.1 cm thick high-density polyethylene (HDPE) elastic plate as shown in Figure 1. This arrangement of flapping foil was taken from the work reported in [20], where an elastic plate was attached to the leading edge of the foil to guide the hydrofoil oscillate smoothly in waves.

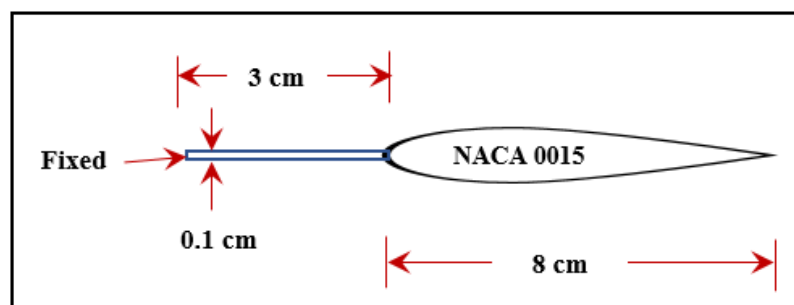


Figure 1. Flapping foil.

FSI simulations for the active and passive mode of flapping foil were done using ANSYS Workbench 19.2 [21]. Since the current version of simulation tool does not support the FSI simulation for 2-Dimensional models, 1 cm thick geometry consists of fluid and solid domain was created for the simulation. Duration of the simulation was 10 s.

2.1. Geometry

Geometrical models of both flapping foil and fluid domain were created as shown in Figure 2. The fluid domain consists of two media (air and water). Length of the rectangle was six times that of the wavelength (λ) and the structural model was placed at 2λ distance from the inlet and 5 cm below

the mean free surface line. Water depth was considered as 40 cm as shown in Figure 2. An elastic plate (0.1 cm thick) was fixed at one end and from another end and was attached to the leading edge of the hydrofoil. The material properties of the hydrofoil and elastic plate were as acrylic glass and HDPE, respectively.

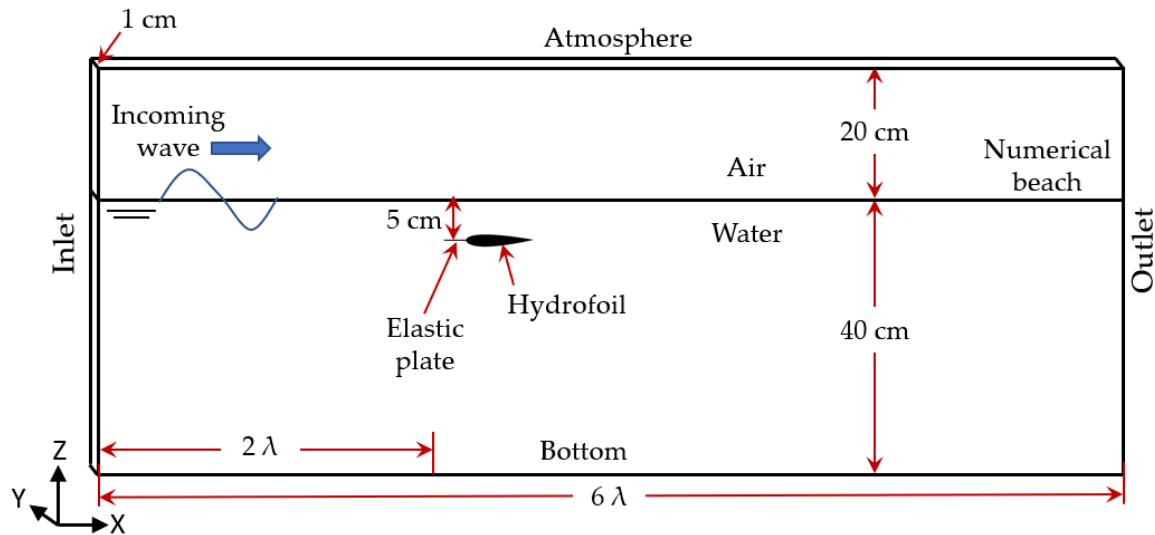


Figure 2. Geometry of fluid domain.

2.2. Computational Mesh

The volume of the fluid domain was formed using FLUENT Mesh. It was made up of tetrahedral cells belonging to the unstructured mesh category. A box of the very fine mesh was created from the inlet to capture the free surface and the structural deformation effectively. Also, the volume mesh of the fluid domain includes the inflation layer around the flapping foil to resolve the boundary layer effects efficiently in turbulent flow as shown in Figure 3. The growth ratio of the inflation layer was 1.2 to maintain a slow transition of meshes. The fluid mesh contained 2.5 million cells.

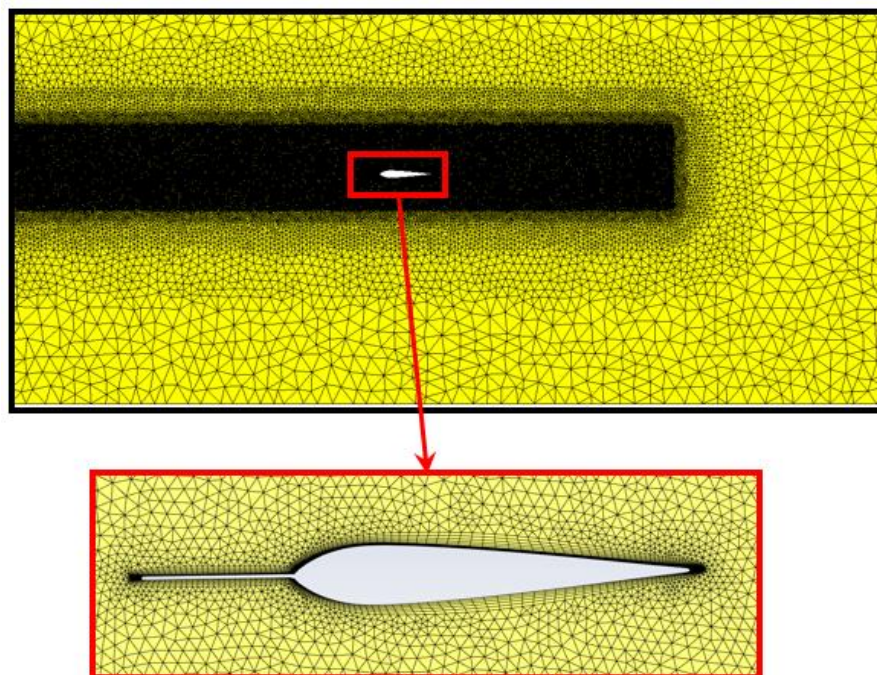


Figure 3. Mesh of fluid domain.

2.2.1. Near Wall Treatment

In order to get a good solution for a wall under dynamic loading, the distance from the wall to the first cell was considered an important parameter, obtained from a non-dimensional number y^+ . The target value of y^+ was evaluated from the ANSYS Fluent simulation as 1. Therefore, the first layer thickness of inflation was evaluated as 0.85 mm.

2.2.2. Structural Mesh

The volume of the solid domain was formed using Structural Mesh. It was made up of hexahedral cells belonging to the structured mesh category as shown in Figure 4. The solid mesh contains 25 thousand cells.

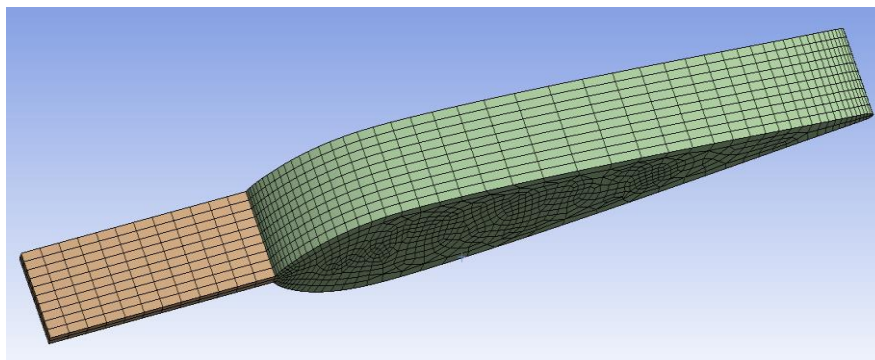


Figure 4. Mesh of solid domain.

2.3. Load Cases

Figure 5 shows the trailing edge displacements of the active flapping foil. The frequency of the five forced flapping and wave specification were displayed in Tables 1 and 2 respectively.

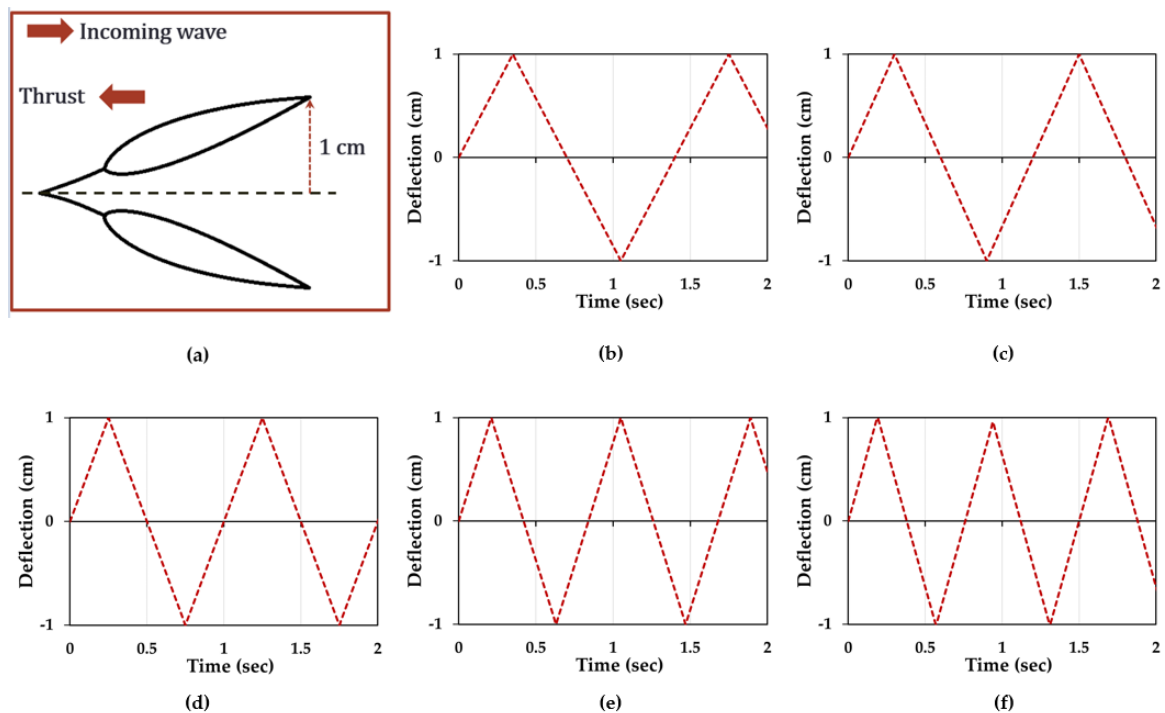


Figure 5. Forced flapping profile. (a) flapping mode; (b) Flap-1; (c) Flap-2; (d) Flap-3; (e) Flap-4; (f) Flap-5.

Table 1. Load cases of active flapping foil.

Load Cases	Flapping Frequency (Hz)	Flapping Period (s)
Flap-1	0.71	1.4
Flap-2	0.83	1.2
Flap-3	1.0	1.0
Flap-4	1.18	0.85
Flap-5	1.33	0.75

Table 2. Wave specification.

Wave	Wavelength (m)	Wave Height (m)
Short wave	0.52	0.02

2.4. Modal Acoustic Analysis

Modal acoustic analysis was performed to determine the natural flapping frequency of the foil in air and water [22] as shown in Figure 6. It was an essential process to avoid any structural failure due to resonance.

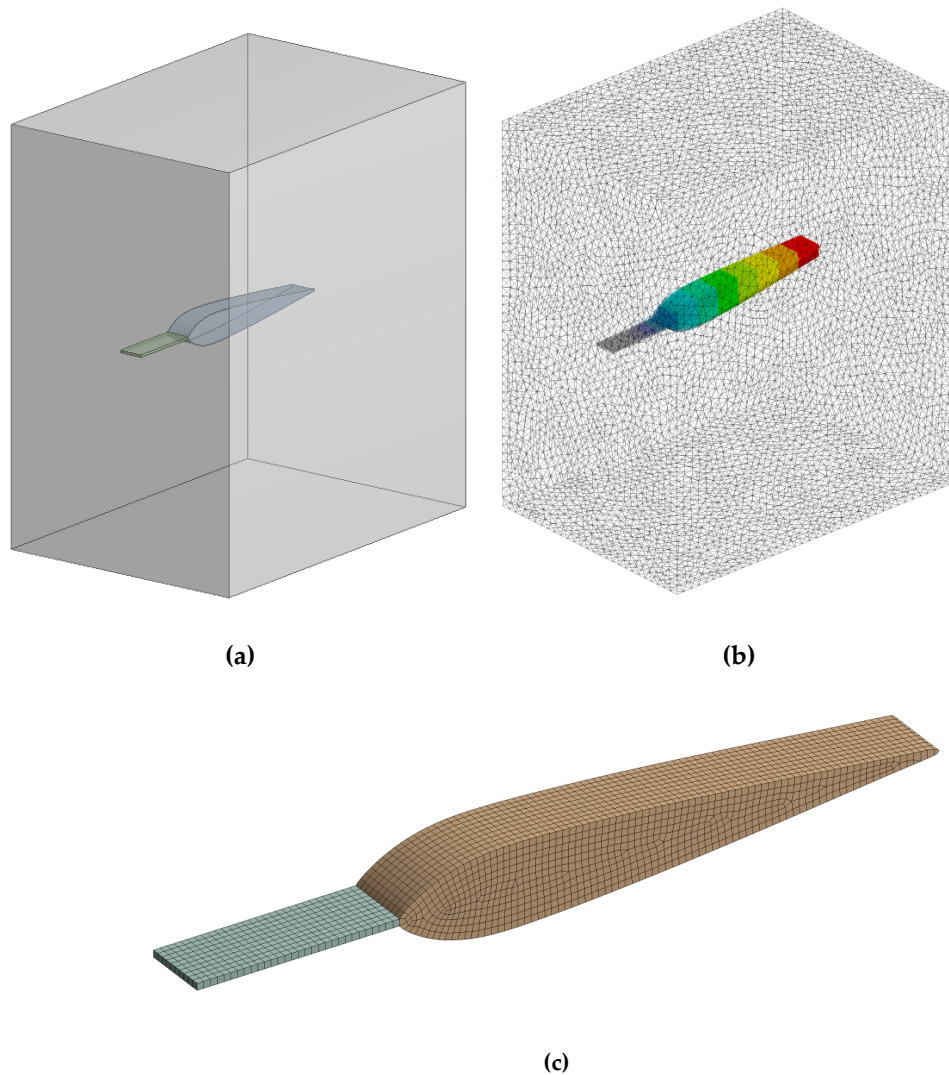


Figure 6. (a) Modelling of modal acoustic body; (b) Meshing of acoustic body; (c) Meshing of flapping foil.

In order to evaluate the natural frequencies of a flapping foil in air and water, an acoustic body of fluid around the flapping foil was created. The used model is shown in Figure 6a. Figure 6b shows the 380,000 tetrahedral mesh generated for the acoustic body and Figure 6c shows the 10,000 hexahedral mesh generated for the solid structure. The interface of solid and acoustic body element nodes was shared to avoid contact elements. The modal acoustic analysis was performed in full damping mode. The natural period of the flapping foil was estimated as 0.15 s in air and 0.23 s in water, that was much smaller than the forced flapping frequency of the foil displayed in Table 1.

2.5. Simulation Setup

The 2-way FSI simulation was conducted to evaluate the thrust forces due to active flapping motion of the hydrofoil in short waves.

2.5.1. Boundary Conditions

Table 3 shows the conditions applied to the boundaries of the fluid domain shown in Figure 2.

Table 3. Boundary conditions of fluid domain.

Domain	Boundary Condition
Inlet	Velocity-inlet (open channel wave boundary)
Outlet	Pressure-outlet (Numerical beach)
Atmosphere	Wall (zero shear)
Flapping Foil	Wall (no slip)
Side wall	Symmetry
Bottom	Wall (zero shear)

2.5.2. FLUENT Solver Setup

Fluent uses the finite volume method to convert the general transport equation into a system of algebraic equations. The Reynolds Averaged Navier Stokes (RANS) was used to model the effects of turbulence. K- ω SST (Shear Stress Transport) turbulence model was used to effectively capture the near the wall flow and free surface flow regions as shown in Table 4.

Table 4. Solver setup.

Air Density	1.225 kg/m³
Water density	998.2 kg/m ³
Turbulence model	k- ω SST
Multiphase model	Volume of fluid
Scheme	implicit
Wave theory	2nd order stokes
Pressure velocity coupling	SIMPLE
Flow	Open channel flow
Momentum	2nd order upwind
Volume fraction	compressive
Pressure	PRESTO
Turbulent kinetic energy (k)	2nd order upwind

2.5.3. System Coupling Setup

System coupling tool was used to integrate fluid and structural solvers in FSI simulations. Figure 7 shows how ANSYS fluid solver (FLUENT) and ANSYS solid solver (MECHANICAL) were coupled and the information transferred.

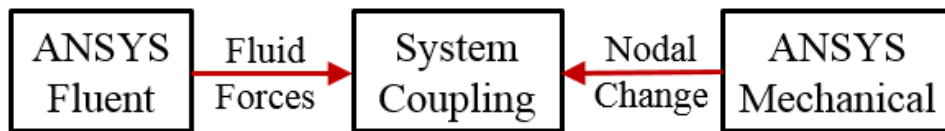


Figure 7. System coupling flow chart.

FLUENT provides information on the fluid forces acting on the body and Mechanical provides nodal displacement changes in the structure due to fluid loading and system coupling synchronize the whole setup of simulation. This type of simulation called 2-way FSI. The step size for the simulation was used as 0.0005 s.

3. Results

Thrust forces obtained for the active mode of the flapping foil in a numerically modelled 1 cm thick fluid–solid domain are shown in Figure 3 and the end effects of the flapping foil was neglected. The span of the flapping foil was 20 cm during the experiment, therefore, all the numerically obtained results were multiplied 20 times and presented in this paper. The global forces acting on the flapping foil in the x-direction of the wave flume were considered as thrust forces. However, in the results section, the thrust forces were varying in the y-direction of the plots. The positive y-direction of the thrust plot represents the force generated against the wave direction.

3.1. Mesh Convergence

In order to perform a mesh convergence study, three mesh resolutions were created as mentioned in Table 5. Mesh convergence check was performed in ANSYS FLUENT 19.2 by generating a regular wave. And the forces acting on the fixed foil in x and z directions were evaluated as shown in Figure 8a,b, respectively.

Table 5. Mesh resolutions.

Mesh Resolution	Number of Elements
Case-1	1.2 million
Case-2	2.5 million
Case-3	4.1 million

Results in Figure 8 show that case 1 was slightly underestimating the peak value. However, case 2 and case 3 show a good agreement therefore, case 2 mesh resolution was selected for the 2-way FSI simulation to save the computation time.

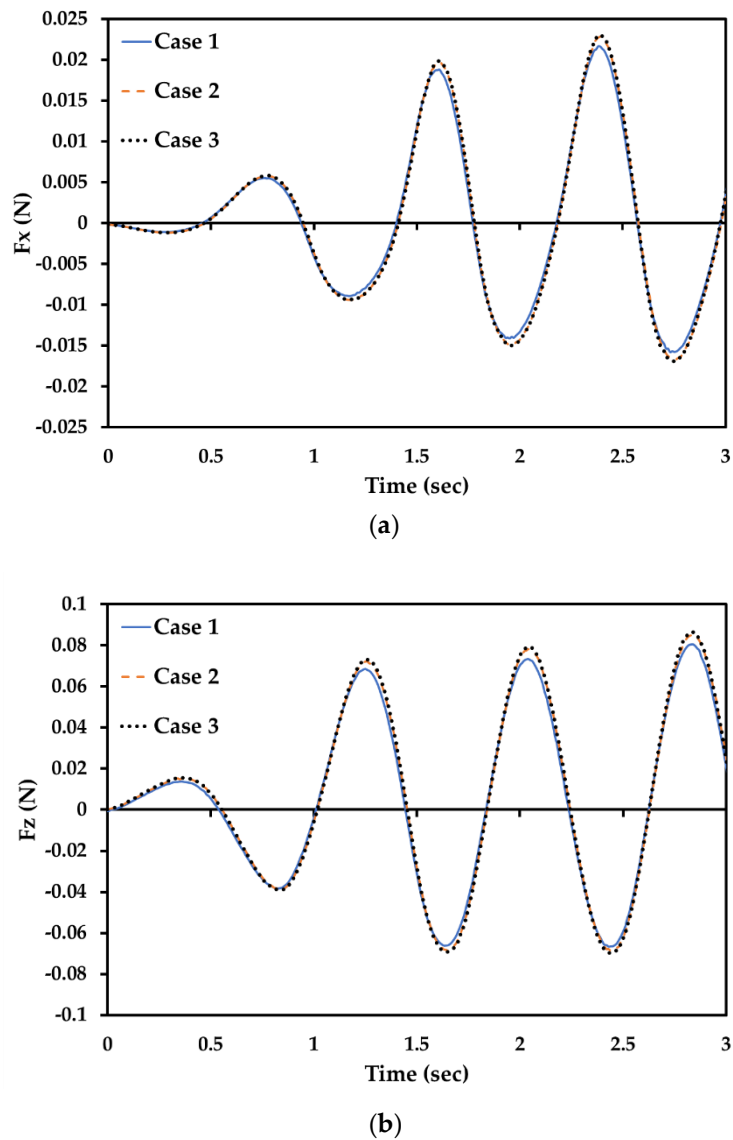
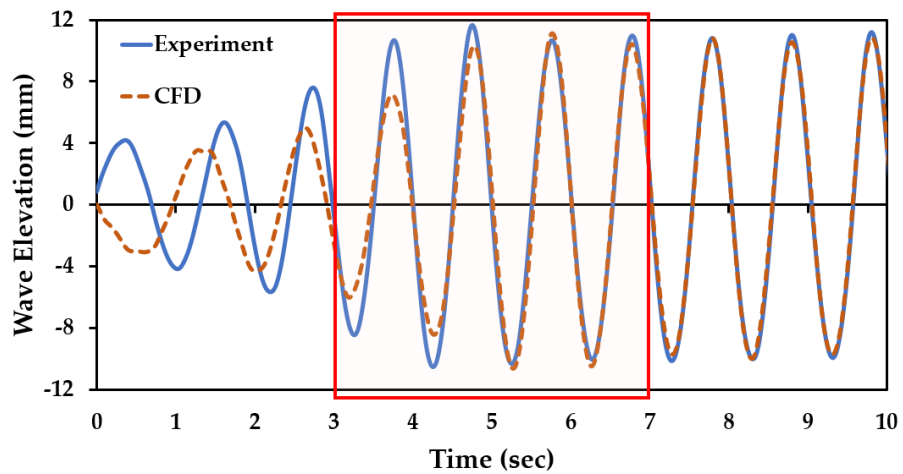


Figure 8. (a) Forces on the fixed foil in x direction; (b) Forces on the fixed foil in z direction.

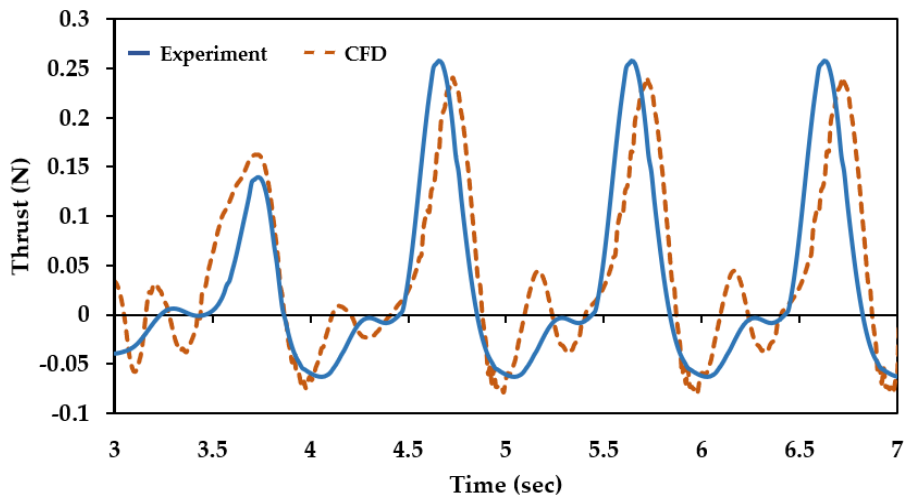
3.2. Validation of Numerical Model

The thrust forces generated by a passive flapping foil were measured experimentally in various waves and elastic conditions and reported in [20]. A CFD simulation of passive flapping foil in waves was compared with the experimentally recorded time series data. Figure 9a shows the comparison of wave profiles from 0 to 10 s. Figure 9b shows the comparison of thrust forces for the highlighted region in Figure 9a, from 3 to 7 s. The comparison of results validates the numerical method qualitatively.

The efficient measurement of thrust forces for the active mode of flapping foil experimentally was complicated, therefore, 2-way FSI with CFD simulation might be used to evaluate thrust and other hydrodynamic properties.



(a)



(b)

Figure 9. (a) Wave profile comparison; (b) Thrust force comparison.

3.3. Fixed Hydrofoil

For the incident short wave displayed in Table 2, an experiment was carried out for a fixed foil to capture the thrust forces measured in the x-direction as shown in Figure 10, therefore, 1 mm thick HDPE elastic plate was replaced by a rigid stainless steel plate of same thickness and sinusoidal variation of force in the surge (F_x) was recorded and compared with the numerically evaluated results using CFD.

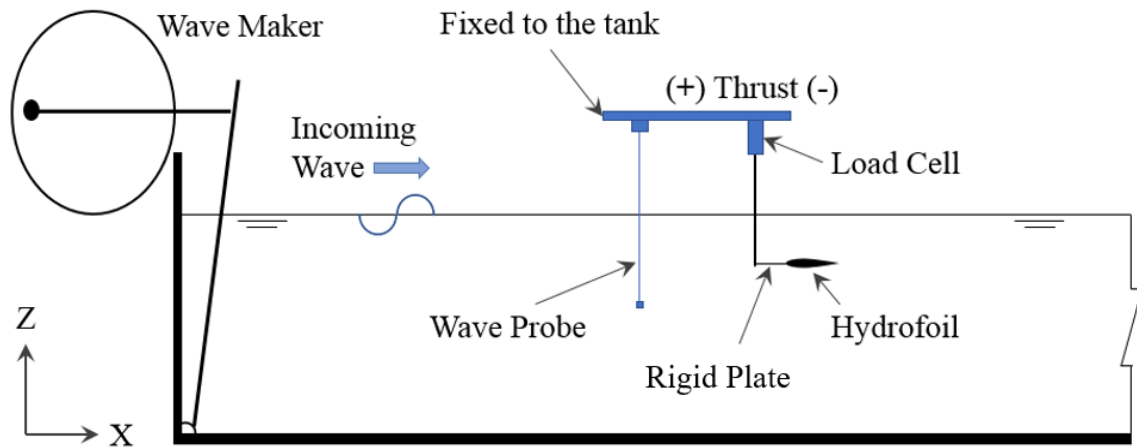


Figure 10. Experimental setup to measure F_x for a fixed hydrofoil in short waves.

Figure 11a,b show the comparison of wave elevations and the pressure force variations on the fixed foil in time domain respectively. The CFD numerical results were in good agreement with experimental data.

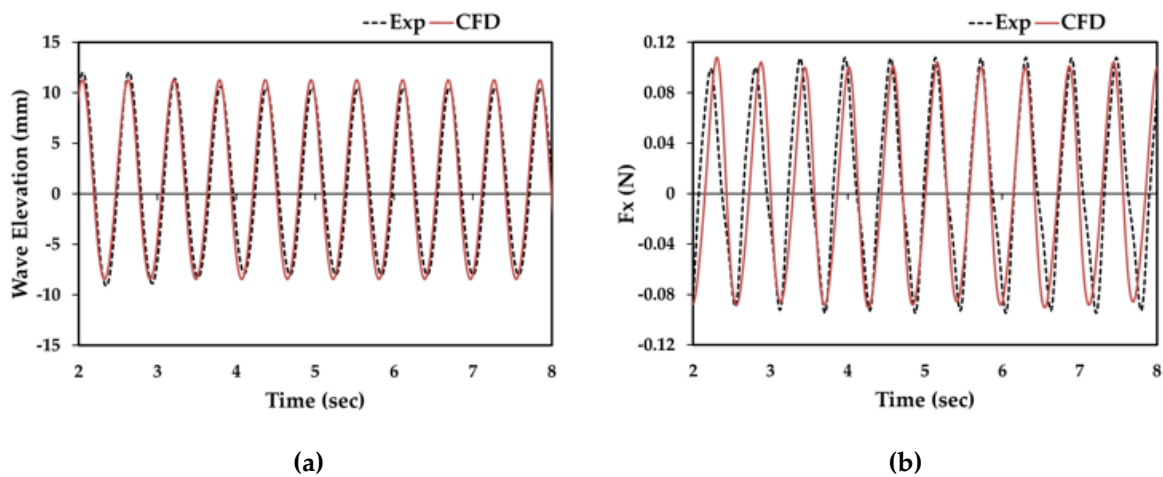


Figure 11. Comparison of experimental and CFD results (a) Wave elevation; (b) Force (F_x).

3.4. Flapping in Still Water

Thrust forces generated by the active flapping foil in still water with five flapping frequencies were evaluated using CFD-FSI simulation. Figure 12a–e show the thrust plots with the trailing edge deflection of the hydrofoil for flap-1, flap-2, flap-3, flap-4 and flap-5, respectively.

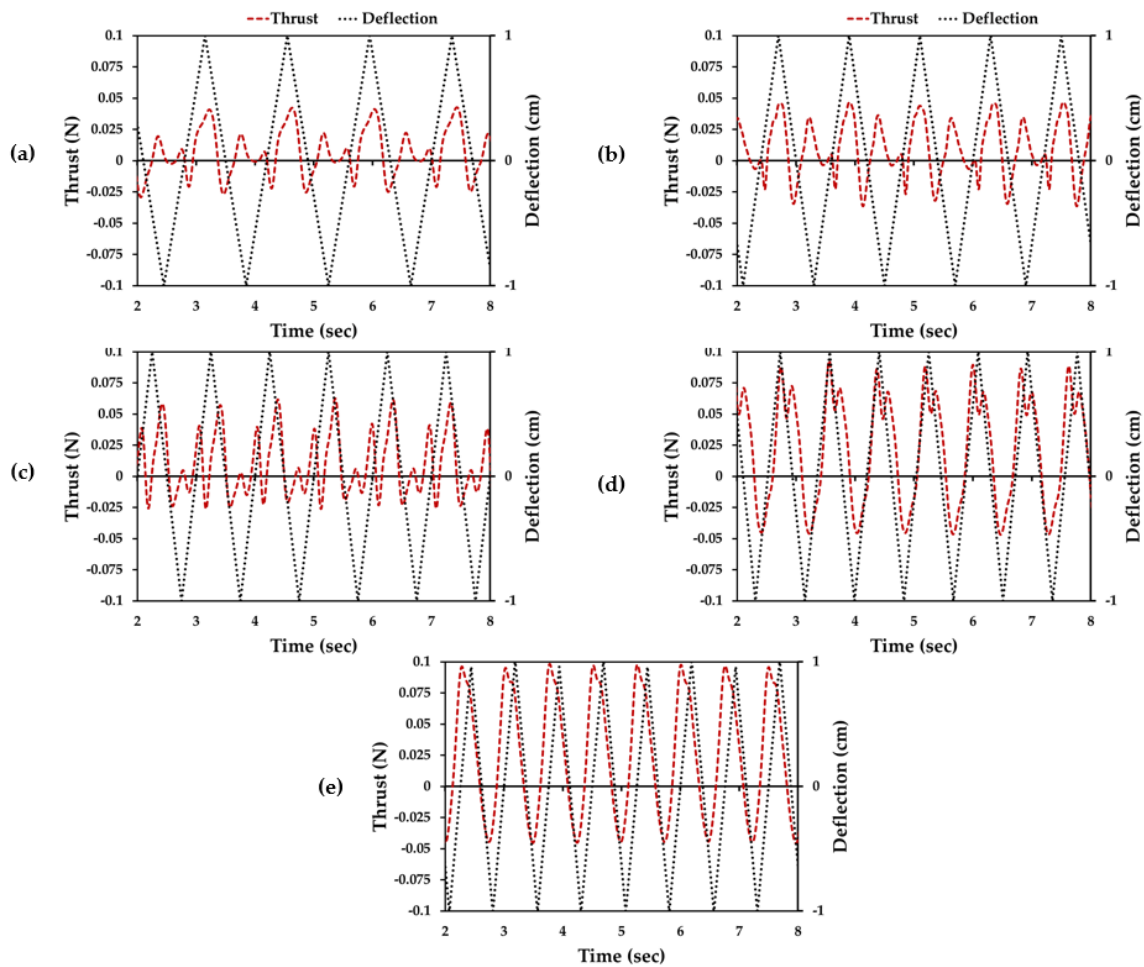


Figure 12. Thrust plot in still water using CFD (a) Flap-1; (b) Flap-2; (c) Flap-3; (d) Flap-4; (e) Flap-5.

Results prove that the thrust forces can be generated by the active flapping motion of the foil in still water. As the flapping frequency increased, the magnitude of thrust forces increased, however, the number of thrust peaks decreased.

3.5. Active Mode Results in Short Wave

Finally, five active modes of flapping foil were simulated in a short wave using 2-way FSI simulation and the results are displayed in Figure 13b–f for flap-1, flap-2, flap-3, flap-4, and flap-5 respectively. Results show that the magnitude of thrust forces increased drastically in active mode with waves compared to active mode in still water and fixed hydrofoil in waves, due to its ability to convert wave energy into propulsive energy, a fixed foil could not create an effective angle of attack to efficiently transform the wave energy into propulsive energy, and in still water conditions, there was a no incoming wave or fluid flow to generate lift and thrust forces for the angle of attacks created by the active flapping. However, 2-way FSI analysis could couple the effects of waves with active flapping; therefore, higher thrust peaks were evaluated.

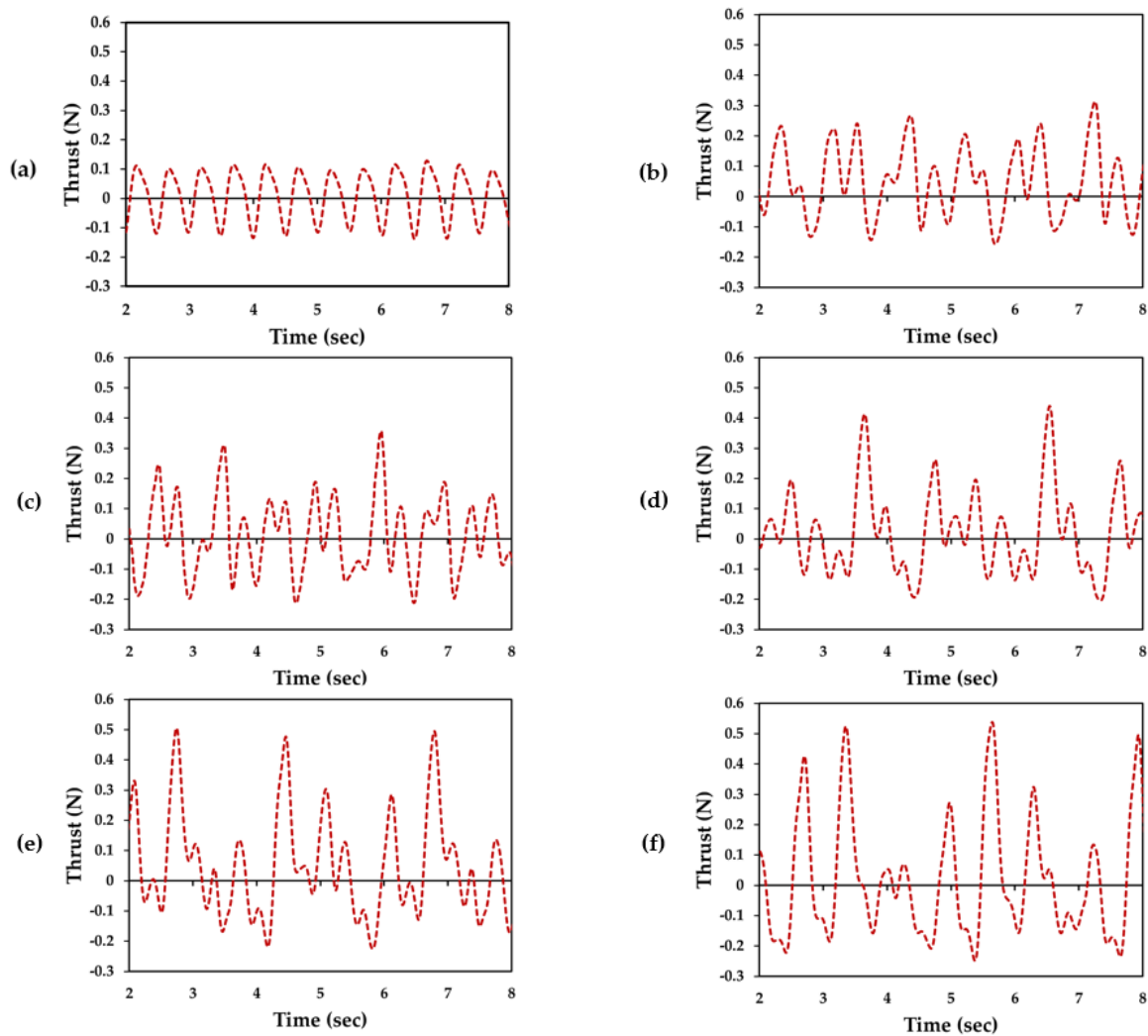


Figure 13. Thrust plot in short waves (a) Passive flapping foil (Experiment); (b) Flap-1 (CFD); (c) Flap-2 (CFD); (d) Flap-3 (CFD); (e) Flap-4 (CFD); (f) Flap-5 (CFD).

Figure 13a shows the experimentally measured thrust data of passive flapping foil in a short wave specified in Table 2. In the passive mode, there was no significant difference in the positive and negative thrust peaks, hence it was not enough to prevent the floater from drifting during the station-keeping tests [21]. Conversely, Active modes were dominating in the positive side of the thrust plots. Therefore, active flapping foil could be a potential solution for the station-keeping problems in the short waves.

4. Conclusions

In this study, 2-way FSI with CFD simulation was used to evaluate the thrust forces generated by the active and passive flapping foils in short wave and still water conditions. Also, the numerical method was validated by making comparisons with experimentally recorded data in passive flapping foil and fixed foil modes. Simulation results confirmed the generation of thrust forces due to the flapping motion of foil in both active and passive modes. Foils were flapping at a set location and generating thrust forces against the direction of incoming waves, which was vital for the design of the station-keeping system of a floater in waves.

Results proved that the active flapping can generate thrust forces for the station-keeping of a floater in short waves. The magnitude of thrust forces can be controlled by adjusting the flapping

frequency of the foil, and for further development of the flapping foil station-keeping system, CFD can be a very efficient tool to evaluate the dynamic behavior of it.

5. Future Research

In the future, the total drag of prototype floater in short waves will be evaluated experimentally and numerically. Drag forces must be neutralized by generating an equal amount of thrust forces to achieve station-keeping goals. The present study would be useful in designing the number of foils to be installed and corresponding flapping frequencies based on motor capacity. Further, a controller will be developed to keep the floater drift within the allowable limit. Finally, the active mode station-keeping prototype setup will be examined in the laboratory and open sea conditions.

Author Contributions: Conceptualization, validation, R.K. and H.S.; methodology, software, writing—original draft preparation, R.K.; writing—review and editing, supervision, H.S.

Funding: This research was supported by the Korea Institute of Energy Technology Evaluation and Planning (KETEP) grant funded by the Korea government (MOTIE) (20184030202280) and by Korea Electric Power Corporation (R18XA03).

Conflicts of Interest: The authors declare no conflict of interest. The funders had no role in the design of the study; in the collection, analyses, or interpretation of data; in the writing of the manuscript, or in the decision to publish the results.

References

1. Licht, S.; Hover, F.; Triantafyllou, M.S. Design of a Flapping Foil Underwater Vehicle. In Proceedings of the 2004 International Symposium on Underwater Technology (IEEE), Taipei, Taiwan, 20–23 April 2004; pp. 311–316.
2. Evangelos, S.F. Augmenting ship propulsion in waves using flapping foils initially designed for roll stabilization. In Proceedings of the 4th International Young Scientists Conference on Computational Science, Athens, Greece, 25 June–3 July 2015; pp. 103–111.
3. Wu, T. Extraction of flow energy by a wing oscillating in waves. *J. Ship Res.* **1972**, *14*, 66–78.
4. Isshiki, H. A theory of wave devouring propulsion (4th report). *J. Soc. Nav. Arch. Jpn.* **1984**, *151*, 54–64. [[CrossRef](#)]
5. Isshiki, H. A Theory of Wave Devouring Propulsion (2nd Report). *J. Soc. Nav. Arch. Jpn.* **1982**, *1982*, 89–100. [[CrossRef](#)]
6. Freymuth, P. Propulsive vortical signature of plunging and pitching airfoils. *AIAA J.* **1988**, *26*, 881–883. [[CrossRef](#)]
7. Schouveiler, L.; Hover, F.S.; Triantafyllou, M.S. Performance of flapping foil propulsion. *J. Fluids Struct.* **2005**, *20*, 949–959. [[CrossRef](#)]
8. Hover, F.S.; Haugsdal Triantafyllou, M.S. Effect of angle of attack profiles in flapping foil propulsion. *J. Fluids Struct.* **2004**, *19*, 37–47. [[CrossRef](#)]
9. Read, D.A.; Hover, F.S.; Triantafyllou, M.S. Forces on oscillating foils for propulsion and maneuvering. *J. Fluids Struct.* **2003**, *17*, 163–183. [[CrossRef](#)]
10. Yu, J.; Tan, M.; Wang, S.; Chen, E. Development of a biomimetic robotic fish and its control algorithm. *IEEE Trans. Syst. Man. Cybern.* **2004**, *34*, 1789–1810. [[CrossRef](#)]
11. Fish, F.E. Advantages of Natural Propulsive Systems. *Mar. Technol. Soc. J.* **2013**, *47*, 37–44. [[CrossRef](#)]
12. Woolim, S.; Rupesh, K.; Youngjae, Y.; Junbae, K.; Beongcheon, S.H. Experimental study of the stationkeeping system of a floater using flapping foils in waves. In Proceedings of the 8th PAAMES and AMEC, Busan, Korea, 9–12 October 2018; pp. 359–362.
13. Nematbakhsh, A.; Bachynski, E.E.; Gao, Z.; Moan, T. Comparison of wave load effects on a TLP wind turbine by using computational fluid dynamics and potential flow theory approaches. *Appl. Ocean Res.* **2015**, *53*, 142–154. [[CrossRef](#)]
14. Bredmose, H.; Jacobsen, N.G. Breaking Wave Impacts on Offshore Wind Turbine Foundations: Focused Wave Groups and CFD. In Proceedings of the ASME 2010 29th International Conference on Ocean, Offshore and Arctic Engineering, Shanghai, China, 6–11 June 2010; pp. 397–404.

15. Westphalen, J. Extreme Wave Loading on Offshore Wave Energy Devices Using CFD. Ph.D. Thesis, University of Plymouth, Faculty of Science and Technology, Coimbra, Portugal, 2011.
16. Blocken, B.; Defraeye, T.; Koninckx, E.; Carmeliet, J.; Hespel, P. CFD simulations of the aerodynamic drag of two drafting cyclists. *Comput. Fluids* **2013**, *71*, 435–445. [[CrossRef](#)]
17. Jameson, A. Optimum Aerodynamic Design Using CFD and Control Theory. In Proceedings of the 12th Computational Fluid Dynamics Conference, San Diego, CA, USA, 19–22 June 1995; p. 1729.
18. Lee, B.K. Computational fluid dynamics in cardiovascular disease. *Korean Circ. J.* **2011**, *41*, 423–430. [[CrossRef](#)] [[PubMed](#)]
19. Sun, Z.; Xu, L. Computational fluid dynamics in coronary artery disease. *Comput. Med. Imaging Graph.* **2014**, *38*, 651–663. [[CrossRef](#)] [[PubMed](#)]
20. Kumar, R.; Shin, H. Thrust estimation of a flapping foil attached to an elastic plate using multiple regression analysis. *Int. J. Nav. Arch. Ocean Eng.* **2019**, *11*, 828–834. [[CrossRef](#)]
21. Kane, J.M. *ANSYS FLUENT 12.0 User' Guide*; ANSYS, Inc.: Canonsburg, PA, USA, 2011.
22. Hengstler, J. Influence of the Fluid-Structure Interaction on the Vibrations of Structures. Ph.D. Thesis, Eidgenössische Technische Hochschule Zürich (ETH), Zurich, Switzerland, 2013.



© 2019 by the authors. Licensee MDPI, Basel, Switzerland. This article is an open access article distributed under the terms and conditions of the Creative Commons Attribution (CC BY) license (<http://creativecommons.org/licenses/by/4.0/>).